Chapter

Dynamic Range Enhancement in Swept-Source Optical Coherence Tomography

Jun Zhang, Xinyu Li and Shanshan Liang

Abstract

The imaging penetration depth of an optical coherence tomography (OCT) system is limited by the dynamic range of the system. In a common case that signals exceed the dynamic range of a Fourier domain OCT (FDOCT) system, saturation artifacts degrade the image quality. In this chapter, we demonstrate some new cost-effective techniques to improve the dynamic range of a swept-source OCT (SSOCT) system. For example, one method is based on a dual-channel detection technique to enhance the dynamic range by reconstructing the saturated signals due to strong reflection of the sample surface. Another method utilizes a tunable high-pass filter to compensate the attenuation of light signal in deep tissue. It was demonstrated that these techniques can improve the dynamic range of an SSOCT system by more than 10 dB with a low bit-depth analog-to-digital converter.

Keywords: saturation artifacts, dynamic range, dual-channel detection, attenuation compensation, endoscopic OCT, contrast

1. Introduction

As a noninvasive, high-resolution tomographic technique providing cross-sectional and three-dimensional imaging of biological tissue in micrometer scale, optical coherence tomography (OCT) has been widely used in many clinical applications including ophthalmology [1], dermatology, interventional cardiology imaging, airway imaging [2, 3], etc.

Compared to time domain OCT (TDOCT), Fourier domain OCT (FDOCT) can achieve a much higher sensitivity and imaging speed [4]. Using the Fourier domain technique based on a high-speed wavelength swept source, swept-source OCT (SSOCT) is capable of an A-line rate of up to multi-MHz [5] with a simple fiber-based setup, which makes SSOCT attractive in clinical applications especially in endoscopic imaging of internal organs [6, 7].

In spite of all the advantages of SSOCT, there are still some impediments that degrade the image quality especially in in vivo endoscopic studies. One of the challenges is the saturation effects due to the strong signals from highly reflective areas such as surface of internal organs that are commonly lubricated by mucus, catheters and guide wires assembled in endoscopic probes, metallic stent struts and micro-calcifications, etc. Since the incident angle is hard to control in endoscopic OCT imaging, the power of the reflected signal light occasionally exceeds the input range of the detector or analog-to-digital converter (ADC). Fourier transformation of the saturated signal results in a bright line on the tissue surface accompanied with a band of artifacts across tissue depth that degrades the image quality and leads to complete loss of information in the areas with strong artifacts.

One solution is to increase the input range of the detector or ADC especially the latter since the limited bit depth of the ADC is usually the bottleneck of the dynamic range of the system. However, a high-performance ADC with a high bit depth and high sampling frequency is costly. Huang et al. reported a method to correct saturation artifacts by linear interpolation of the signals in adjacent A-lines [8]. However, the interpolation-based reconstruction can only be used in the correction of sparse saturation artifacts. An adaptive optimization technique based on automatic adjustment of the reference power was used to suppress saturation effects in spectral-domain OCT (SDOCT) [9] at the cost of significantly slowing down the frame rate due to complex design and calculations. Wu et al. utilized a multi-exposure spectrum recording method to reduce saturation artifacts in SDOCT [10]. However, the compensation effect was limited by the inaccurate estimation of the multi-exposure signal levels since the ratio of the levels cannot be precisely calibrated. Therefore, a real-time and accurate technique to correct saturation effect suited for SSOCT systems especially in endoscopic imaging is still absent.

An alternative design based on a dual-channel detection technique was presented to suppress the saturation artifacts [11]. The detected signal was split into the two channels with the ratio of the signal levels precisely calibrated. The high-level signal was used to reconstruct OCT images, and the low-level signal was used to correct the saturated signal in the case that the high-level signal exceeds the input range of the system. This technique allows for a simple and cost-effective suppression of saturation artifacts in endoscopic SSOCT without the need of decreasing the incident power.

Another impediment that degrades the image quality of OCT is that image contrast decays drastically with imaging depth due to strong attenuation of light in biological tissues [12]. Chang et al. reported a method to compensate OCT signal attenuation in depth by adaptively deriving a compensation function for each A-scan line [13]. Hojjatoleslami et al. proposed an enhancement algorithm for attenuation compensation to improve the image quality in the structures at deeper levels [14]. Zhang et al. built a dual-band FDOCT system and developed an algorithm to compensate depth-related discrepancy and attenuation [15]. An alternative approach of compensating attenuation by performing extraction of optical scattering parameters was presented by Anderson et al. [16, 17]. Girard et al. developed a series of algorithms that can be applied to compensate light attenuation and enhance contrast in both time and spectral-domain OCT images [18]. However, these algorithm-based approaches require a prohibitive number of computations and are not practical for real-time imaging. Recently, Li et al. combined a tunable high-pass filter with a dual-channel ADC to compensate signal decay in deep tissue in real time [19]. Since signal frequency represents the depth in SSOCT imaging, low-frequency signal in one channel that is filtered out by a high-pass filter and then combined with the signal in the other channel can be used to reconstruct a high-contrast image in both surface and deep area of the tissue.

2. Correction of saturation effects

The schematic diagram of the SSOCT system for correction of saturation effects is shown in **Figure 1** [11]. A swept source at 1310 nm with a bandwidth of 87 nm, a sweep frequency of 100 kHz, and an output power of 20 mW were used as the light source. The input light was split by a 1 × 2 coupler into the sample and reference arms, respectively. In the sample arm, a 1.3 mm proximal scanning endoscopic probe was employed for three-dimensional imaging. The helical scanning probe was driven by a rotary motor with a rotational rate of 50 rounds/seconds and a stepper motor translational stage with a pulling-back speed of 1 mm/second, respectively. By using a phase-resolved algorithm to computationally compensate the dispersion generated by the endoscope optics, the SSOCT system is capable of an axial resolution of 8 μm in the tissue and a lateral resolution of 20 μm, respectively. The total reference power was set to be 25 μW for optimization of the system sensitivity. In the detection arm, a balanced detector with the noise level comparable to the quantization noise of the ADC was used. In order to compensate saturation artifacts, the interference signal was divided into two paths by a broadband power divider and then digitized by a 12-bit two-channel ADC. In each channel, 1024 samples were acquired using the k-clock from the laser source as an external clock signal. The splitting ratio of the power divider was accurately calibrated by utilizing a high-performance oscilloscope. The signal collected by the high-level channel (ChA) was used for OCT imaging. To detect saturation in ChA, a threshold of the low-level signal in ChB was set to be equal to the input range divided by the splitting ratio of the power divider. Hence, the saturated signal in ChA over the maximum input range can be reconstructed with the signal spontaneously detected in ChB. By multiplying the splitting ratio with the signal in ChB, the saturated signal due to strong reflection was compensated as shown in **Figure 2A**. The corresponding

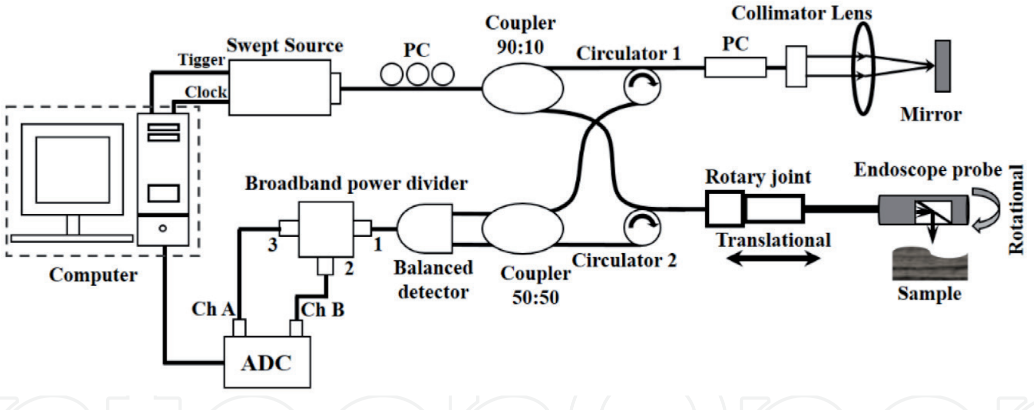

Figure 1.
Schematic of the SSOCT system for saturation correction: PC, polarization controller; ADC, analog to digital converter [11].

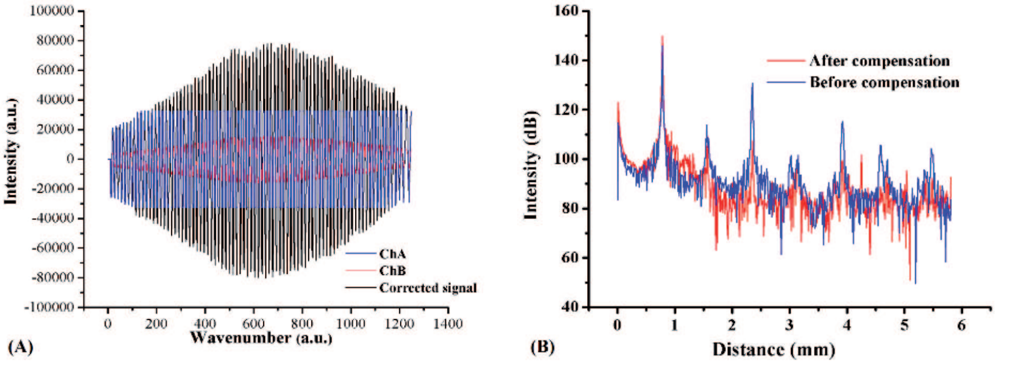

Figure 2.
(A) Interference signals recorded with ChA (blue) and ChB (red). Black line denotes corrected signals in ChA after compensation with signals in ChB. (B) Fourier transforms of signals before and after compensation.

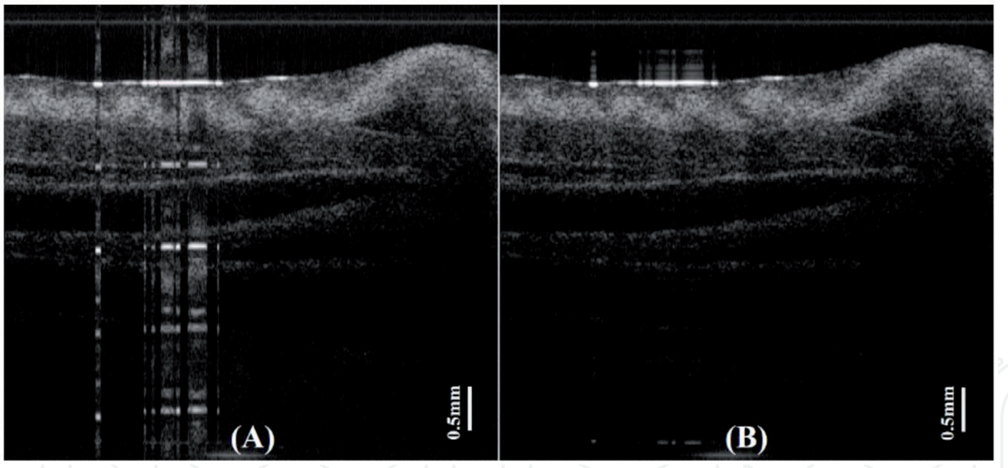

Figure 3.
OCT images of porcine airway before (A) and after (B) correction [11].

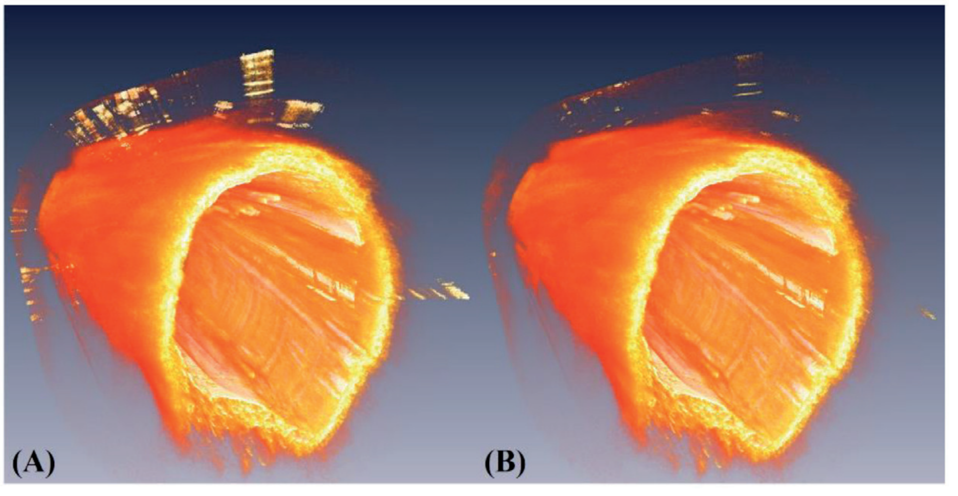

Figure 4.
3D endoscopic OCT images of porcine airway before (A) and after (B) correction.

artifact peaks in depth domain after Fourier transformation were significantly suppressed (**Figure 2B**).

To evaluate the system's capacities of imaging tissues with high reflectivity, a section of porcine upper airway tissues was imaged using the saturation-correction system. OCT imaging was processed on a graphical processing unit (GPU) featuring a multithreaded real-time data acquisition, image processing, and display at the rate of 50 frames/second with 2000 A-lines in each frame. As illustrated in **Figure 3**, the structures hidden inside the bright vertical lines were revived through significant suppression of saturation artifacts [11].

Construction of 3D data sets from 500 B scan utilized a commercial software package. As shown in **Figure 4**, the artifacts were removed with this technique resulting in a clean 3D reconstruction of endoscopic OCT imaging.

3. Compensation of signal attenuation

Figure 5 illustrates the averaged intensity of 1000 A-lines in SSOCT imaging of the human skin showing that signal frequency represents depth in the sample. Hence, attenuated signals in high frequency can be compensated in frequency domain by using a tunable high-pass filter to filter out the low-frequency signal. **Figure 6** shows the frequency response of the high-pass filter with a cutoff frequency set to be 13 MHz.

Figure 7 shows the SSOCT system for attenuation compensation [19]. A swept source with a center wavelength of 1310 nm, a bandwidth of 108 nm, a sweep frequency of 50 kHz, and an output power of 20 mW were used as the light source. The light was split into the sample arm and the reference arm by a 90:10 coupler. The light back-scattered/back-reflected from the reference mirror and sample arm was redirected by two circulators and detected by a balanced detector. The detected signal was divided into two channels of an ADC by a directional coupler with the ratio of 1:5. A high-pass filter was utilized to remove the low-frequency component from the higher-level signal in ChB so that the signal intensity in ChB is close to that in ChA. Since the higher-frequency signals experience stronger attenuation, signals in ChB and ChA can be used to reconstruct structure in deep tissue and surface, respectively. The signals in two channels were combined in real time after being digitized by the ADC.

The human finger was imaged to test the capability of the system to improve the image contrast. As illustrated in **Figure 8**, OCT image after compensation shows an obvious enhancement of contrast in deep area.

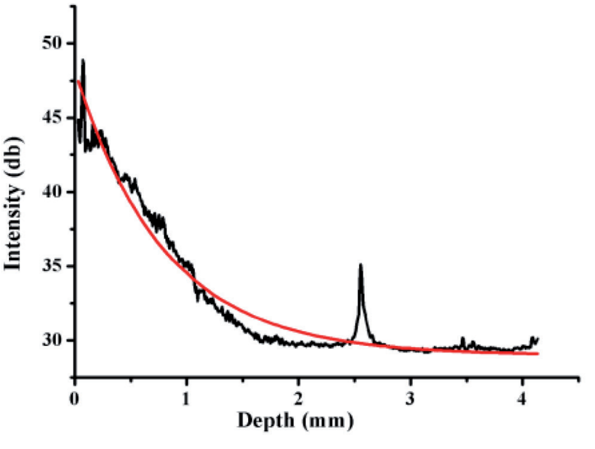

Figure 5.
Averaged intensity of 1000 A-lines in human skin imaging.

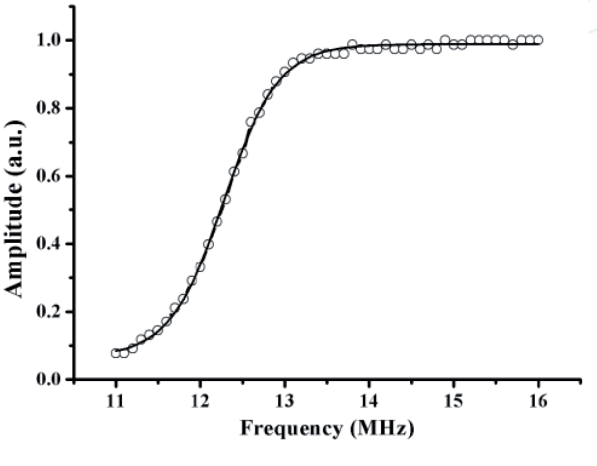

Figure 6.
Frequency response of the high-pass filter.

Porcine upper airway imaging shown in **Figure 9** demonstrated that this method can be used to improve OCT image quality effectively [19].

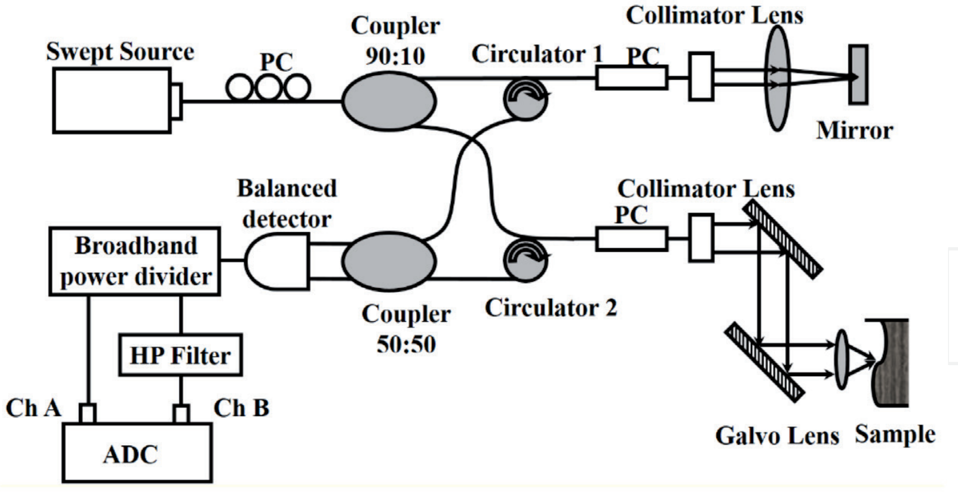

Figure 7.
Schematic of the SSOCT system for attenuation compensation: ADC, analog-to-digital converter.

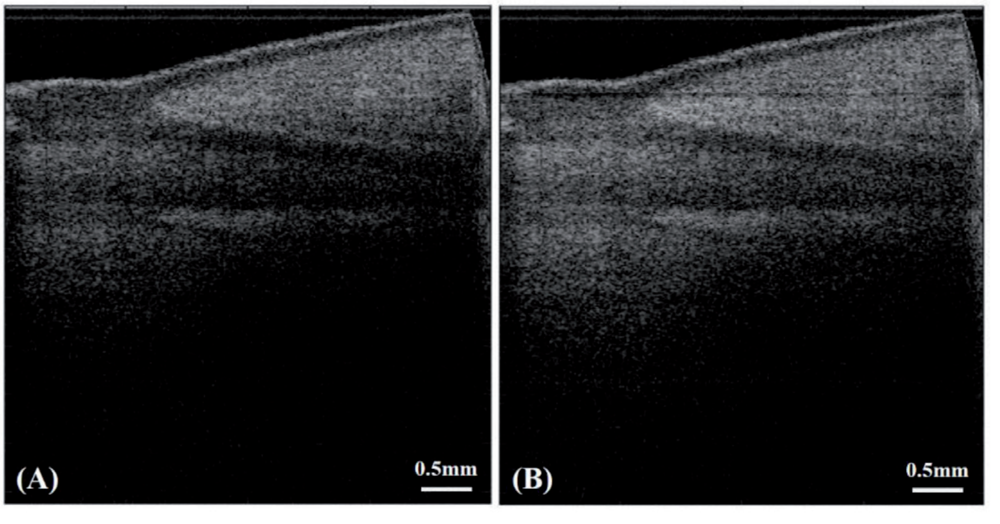

Figure 8.
OCT images of the human finger before (A) and after (B) compensation.

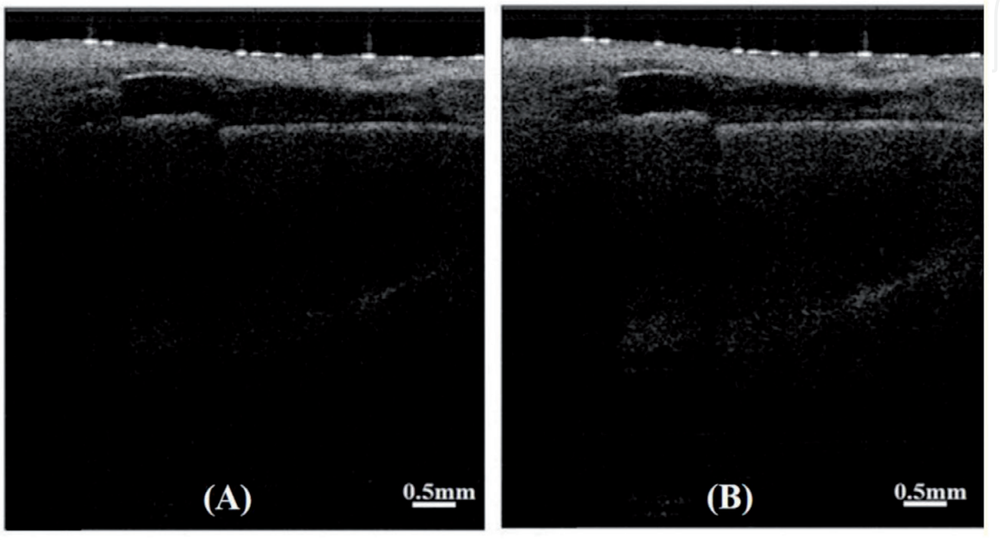

Figure 9.
OCT images of porcine upper airway before (A) and after (B) compensation [19].

4. Conclusions

In clinical applications such as dermatological imaging, the reflectivity of dry tissue is less than 10^{-4}. However, in endoscopic imaging applications, the reflectivities of mucous fluid, catheters, and stent struts usually exceed 10^{-2} or more, resulting in saturation artifacts in OCT images. Increasing the number of bits of an ADC could reduce saturation effects, however requiring complex and costly design. The dual-channel-based saturation-correction approach provides a simple and cost-effective method to solve this problem. The results showed this technique effectively suppresses saturation artifacts especially in endoscopic OCT imaging.

Due to strong attenuation of light in biological tissues, OCT signal decreased dramatically with the penetration depth. The attenuation compensation approach combining a tunable high-pass filter with a dual-channel ADC enhances the contrast of OCT images in a deeper region effectively. Human finger and porcine upper airway imaging demonstrated that high-quality image can be obtained with this method.

In conclusion, the dynamic range of an SSOCT system can be improved by more than 10 dB with a low bit-depth analog-to-digital converter by using these techniques.

Author details

Jun Zhang*, Xinyu Li and Shanshan Liang
School of Electronics and Information Technology, Sun Yat-sen University, Guangzhou, China

*Address all correspondence to: junzhang8819@gmail.com

References

[1] Costa RA, Skaf M, Melo LAS, et al. Retinal assessment using optical coherence tomography. Progress in Retinal and Eye Research. 2006;**25**(3):325-353. DOI: 10.1016/j.preteyeres.2006.03.001

[2] Sinclair H, Bourantas C, Bagnall A, et al. OCT for the identification of vulnerable plaque in acute coronary syndrome. JACC: Cardiovascular Imaging. 2015;**8**(2):198-209. DOI: 10.1016/j.jcmg.2014.12.005

[3] Milne S, King GG. Advanced imaging in COPD: Insights into pulmonary pathophysiology. Journal of Thoracic Disease. 2014;**6**(11):1570-1585. DOI: 10.3978/j.issn.2072-1439.2014.11.30

[4] Leitgeb R, Hitzenberger CK, Fercher AF. Performance of Fourier domain vs. time domain optical coherence tomography. Optics Express. 2003;**11**(8):889-894. DOI: 10.1364/OE.11.000889

[5] Huo T, Wang C, Zhang X, et al. Ultrahigh-speed optical coherence tomography utilizing all-optical 40 MHz swept-source. Journal of Biomedical Optics. 2015;**20**(3):30503. DOI: 10.1117/1.JBO.20.3.030503

[6] Gabriel S. In vivo endoscopic optical coherence tomography of the human gastrointestinal tract - toward optical biopsy. Endoscopy. 2000;**32**(10):743-749. DOI: 10.1055/s-2000-7711

[7] Lee SW, Heidary AE, Yoon D, et al. Quantification of airway thickness changes in smoke-inhalation injury using in-vivo 3-D endoscopic frequency-domain optical coherence tomography. Biomedical Optics Express. 2011;**2**(2):243-254. DOI: 10.1364/BOE.2.000243

[8] Huang Y, Kang JU. Real-time reference A-line subtraction and saturation artifact removal using graphics processing unit for high-frame-rate Fourier-domain optical coherence tomography video imaging. Optical Engineering. 2012;**51**(7):3203. DOI: 10.1117/1.OE.51.7.073203

[9] Kim JH, Han JH, Jeong J. Adaptive optimization of reference intensity for optical coherence imaging using galvanometric mirror tilting method. Optics Communications. 2015;**351**:57-62. DOI: 10.1016/j.optcom.2015.04.041

[10] Wu CT, Tsai MT, Lee CK. Two-level optical coherence tomography scheme for suppressing spectral saturation artifacts. Sensors. 2014;**14**(8):13548-13555. DOI: 10.3390/s140813548

[11] Li X, Liang S, Zhang J. Correction of saturation effects in endoscopic swept-source optical coherence tomography based on dual-channel detection. Journal of Biomedical Optics. 2018;**23**(3):1. DOI: 10.1117/1.JBO.23.3.030502

[12] Jansonius NM, Cervantes J, Reddikumar M, et al. Influence of coherence length, signal-to-noise ratio, log transform, and low-pass filtering on layer thickness assessment with OCT in the retina. Biomedical Optics Express. 2017;**7**(11):4490. DOI: 10.1364/BOE.7.004490

[13] Chang S, Flueraru C, Mao Y, et al. Attenuation compensation for optical coherence tomography imaging. Optics Communications. 2009;**282**(23):4503-4507. DOI: 10.1016/j.optcom.2009.08.030

[14] Hojjatoleslami A, Avanaki MRN. OCT skin image enhancement through attenuation compensation. Applied Optics. 2012;**51**(21):4927-4935. DOI: 10.1364/AO.51.004927

[15] Zhang M, Ma L, Yu P. Dual-band Fourier domain optical coherence tomography with depth-related compensations. Biomedical Optics Express. 2014;**5**(1):167. DOI: 10.1364/BOE.5.000167

[16] Thrane L, Frosz MH, Jørgensen TM, et al. Extraction of optical scattering parameters and attenuation compensation in optical coherence tomography images of multilayered tissue structures. Optics Letters. 2004;**29**(14):1641-1643. DOI: 10.1364/OL.29.001641

[17] Thrane L, Yura HT, Andersen PE. Analysis of optical coherence tomography systems based on the extended Huygens-Fresnel principle. Journal of the Optical Society of America A. 2000;**17**(3):484-490. DOI: 10.1364/JOSAA.17.000484

[18] Girard MJA, Strouthidis NG, Ethier CR, et al. Shadow removal and contrast enhancement in optical coherence tomography images of the human optic nerve head. Investigative Ophthalmology & Visual Science. 2011;**52**(10):7738. DOI: 10.1167/iovs.10-6925

[19] Li X, Liang S, Zhang J. Contrast improvement for swept-source optical coherence tomography image of sub-surface tissue. In: Optical Coherence Tomography and Coherence Domain Optical Methods in Biomedicine XXI. International Society for Optics and Photonics. 2017;**10053**:100532R. DOI: 10.1117/12.2251650